

Fabrication of microprisms for planar optical interconnections by use of analog gray-scale lithography with high-energy-beam-sensitive glass

Christiane Gimkiewicz, Detlev Hagedorn, Jürgen Jahns, Ernst-Bernhard Kley, and Frank Thoma

For an integrated free-space optical interconnection system we suggest the use of microprisms to achieve large coupling angles at low loss. Prisms were fabricated in photoresist and quartz glass by analog lithography. High-energy-beam-sensitive glass was used as the gray-tone mask. Optical testing of the prisms shows acceptable surface quality and high efficiency (95%). © 1999 Optical Society of America
OCIS codes: 200.4650, 350.3950.

1. Introduction

The next generation of electronic circuitry will feature geometrical dimensions as small as 100 nm and chips with more than 10^8 transistors. For the year 2006, on-chip frequencies of as high as 3 GHz are expected. This development will increase the interconnection density; therefore failure mechanisms like cross talk or electromigration will be enhanced. An increasing attenuation and time delay on the circuit lines will further reduce data reliability.¹

For applications with high data rates parallel optical interconnections have been discussed as a solution to the interconnection bottleneck. In particular, integrated planar free-space optics allows one to implement massively parallel optical interconnections combined with compact packaging.² Active components such as vertical-cavity surface-emitting laser (VCSEL) arrays and detector arrays are mounted onto a transparent substrate by means of hybrid integration technology (Fig. 1). The light travels on a zigzag path from the emitters to the

detectors and is distributed and guided by appropriate micro-optical components.

Light coupling from source to substrate requires either diffractive or refractive components for deflection and collimation. For the fabrication of diffractive elements a multimask lithographic process is necessary for achieving efficient coupling gratings. The diffraction angle and the efficiency depend on the minimum feature size s of the lithographic process. An efficient blazed grating consists of n phase steps ($n > 2$) within one grating period p , with $p = ns$. On the other hand, p is inversely proportional to the sine of the diffraction angle. Obviously, a decreasing period p leads to a higher diffraction angle but, in general, also to a lower efficiency because, for a given minimum feature size, the number of phase levels also has to decrease. Increasing the input power of the emitters to offset the efficiency loss of the optical channel would also result in increased heat dissipation and longer switch-ON-switch-OFF times, thus reducing the capacity of the interconnect. Therefore it is of interest to find alternatives to diffractive coupling elements.

During the past few years analog lithographic techniques have been developed that allow one to generate arbitrary surface profiles. Two possible approaches can be identified: (a) Halftone techniques with binary masks³: Here dithering and projection lithography are used in combination with a thick photoresist with gray-level capabilities. (b) Direct-writing techniques that use a modulated electron or laser beam: Here the writing process can be

C. Gimkiewicz (christiane.gimkiewicz@fernuni-hagen.de), D. Hagedorn, and J. Jahns are with Optische Nachrichtentechnik, Fernuniversität Hagen, Feithstrasse 140, D-58084 Hagen, Germany. E.-B. Kley and F. Thoma are with the Institut für Angewandte Physik, Friedrich-Schiller-Universität Jena, Max-Wein-Platz, 1, D-07743 Jena, Germany.

Received 5 August 1998; revised manuscript received 23 November 1998.

0003-6935/99/142986-05\$15.00/0

© 1999 Optical Society of America

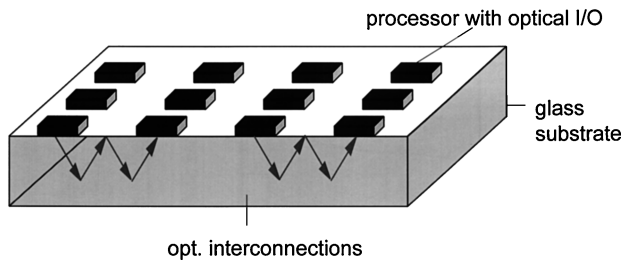


Fig. 1. Integrated planar free-space optical system concept for building compact systems for interconnection and sensor applications. Opt., optical.

used to write directly into the resist⁴ or to generate gray-level masks in high-energy-beam-sensitive (HEBS) glass.⁵ Technique (b) was suggested, in particular, as a mean of simplifying the fabrication of diffractive multilevel elements by a one-step lithographic process. Gray-level lithography is also of interest in combination with surface replication in plastic materials, as was recently demonstrated by Gale *et al.*⁶

In this paper we demonstrate the fabrication of microprism arrays by using the HEBS glass technique. Microprisms are of interest as coupling elements for planar optical interconnects to obtain large coupling angles at high efficiencies. Ultimately, we want to place the prisms on the bottom surface of a GaAs chip with bottom-emitting VCSEL diodes (Fig. 2). A similar approach was taken by Strzelecka *et al.*,⁷ who put refractive microlenses on a VCSEL chip. In our concept separate lenses on the surface of the glass substrate are used to collimate the beam. Alternatively, refractive off-axis lenses could replace a separate arrangement of prisms and lenses.

Here we consider the following situation: A diverging wave emitted from a VCSEL (typically at a wavelength of approximately 980 nm) passes through the GaAs chip before it passes through the prism. The substrate typically has a thickness of a few hundred micrometers. After such a short propagation distance the light beam broadens to a diameter of 50–100 μm , depending on the diameter of the VCSEL and the substrate thickness. Thus prism sizes of the order of 100 μm are of interest. This is the case that is investigated in this paper. The coupling angle introduced by the prism is determined by its wedge

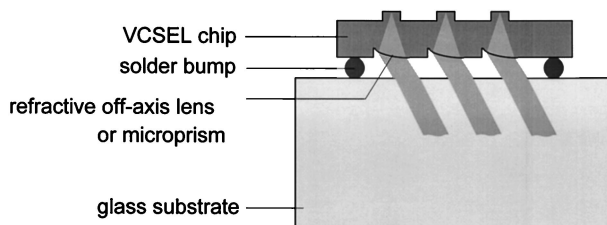


Fig. 2. Use of micro-optical elements in a planar optical interconnect. Microprisms for beam deflection are integrated directly on the bottom surface of the VCSEL chip. Microlenses are used to collimate the beam.

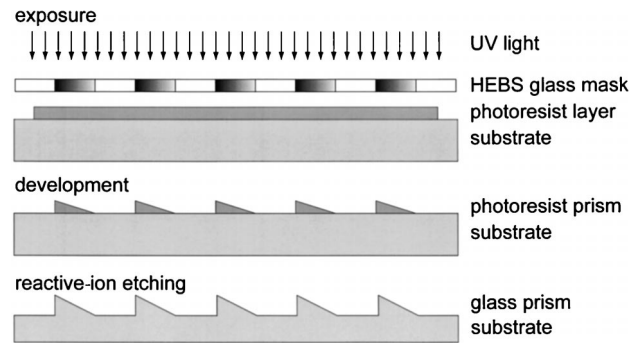


Fig. 3. Analog contact lithography with a HEBS glass gray-scale mask.

angle and the refractive indices. We discuss these issues in Section 4. At this point, we would like to state that coupling angles lying in the range between 20° and 30° are of interest. What we have demonstrated so far and what is described in the following sections is the fabrication of the microprisms in photoresist and glass (Section 2) and optical wave-front and efficiency testing (Section 3). In Section 4 we also briefly discuss the use of the microprisms for planar optical interconnections.

2. Fabrication Process

HEBS glass is a material for use in true gray-level masks.⁸ The fabrication of HEBS glass is an ion-exchange process. Because of a diffusion process the substrate contains silver ions in a surface layer as silver alkali-halide complex crystals.⁵ To avoid reaction by the silver ions to UV light, it is necessary to dope the glass with photoinhibitors. Thus the glass is further sensitive to high-energy beams but does not react to UV exposure. On exposure to a high-energy electron beam (>10 kV) reduction of the silver ions occurs. The electron beam changes the optical density of the glass. The higher the dosage of the beam (typically 0–367 $\mu\text{C}/\text{cm}^2$), the higher the optical density becomes (0–2.6 at an UV wavelength of 365 nm). During the writing process the variable dosage is controlled by a variable dwell time, the acceleration voltage, or the current of the *e*-beam writer. For that reason the gray-scale pattern in the HEBS material can be written in a single step. After the mask is fabricated only one subsequent lithographic step is required to transfer the mask pattern into a three-dimensional photoresist relief (Fig. 3). For fabrication we used AZ4562, which is standard for thick coatings, as the photoresist to be spun onto a quartz-glass substrate. The absorption in AZ4562 is lower than in thin-film resists to provide sufficient energy, even at the bottom of the resist layer, for binary structures. Here the gray levels of the mask prevent the light from penetrating all regions continuously. Different resist depths of soluble materials are generated. A thick resist layer requires a low spin speed, e.g., 800 rpm for a 13- μm -thick layer. After the photoresist baked for an hour on a hotplate at 90 °C, we exposed it with a standard mask aligner at

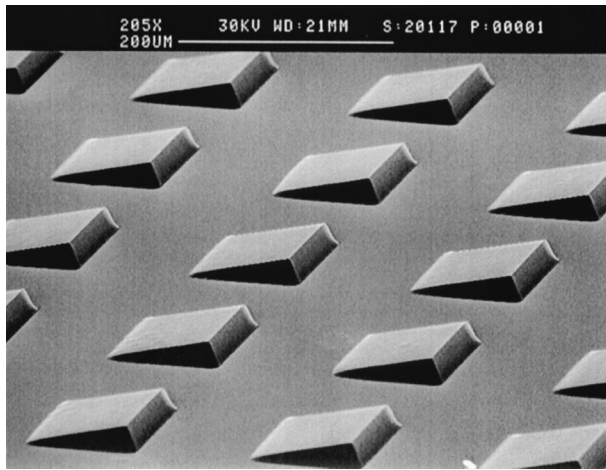


Fig. 4. SEM photograph of a prism array with a 20- μm sag in the photoresist.

a main wavelength of 365 nm. During exposure the evaporation of nitrogen can cause bubbles, thus interval exposures are necessary. For development AZ400K was used. The dissolution of the photoresist is determined by the light intensity transmitted by the patterned HEBS glass. We fabricated prisms with sags ranging from 6 to 20 μm with a base area of 100 $\mu\text{m} \times 100 \mu\text{m}$ (Fig. 4). The surface roughness of a 20- μm -sag prism was determined by an optical profilometer. A rms value of 121 nm was measured for the total prism area, including the marginal zones. A reflow process of the resist prisms with a sag of 6 μm further improved their surface quality. These smoothed photoresist prisms were transferred into quartz by reactive-ion etching (RIE) at an etch rate of 22.5 nm/min. The glass prisms had a height of approximately 4.2 μm .

3. Optical Testing

To test the optical quality of the prisms, we looked at the wave front reflected off a prism, measured the deflection angle of the light beam after passage through the glass substrate, and determined the efficiency of the light transmitted through a prism. In all experiments the maximum beam diameter has to be smaller than or equal to the length of the prism, where a smooth surface can be found. The melting technique slightly decreases the usable prism area. In our experiments the usable length was $l = 82.2 \mu\text{m}$ for the glass prisms, which is an area sufficiently large for our spot diameters of 50 μm . For the wave-front experiments, we used aluminum-coated glass prisms. With our setup, we simultaneously observed the laser spot on the prism surface and the deformation of the wave-front focus after reflection off the prisms with two CCD cameras (Fig. 5). The wave front reflected off a mirror generates the well-known Airy pattern [Fig. 6(a)]. If the mirror is replaced with a coated photoresist prism, the focal spot shows irregularities as a result of the roughness in the prism's surface. In Fig. 6(b) the point-spread function of a photoresist prism with a sag of 20 μm is

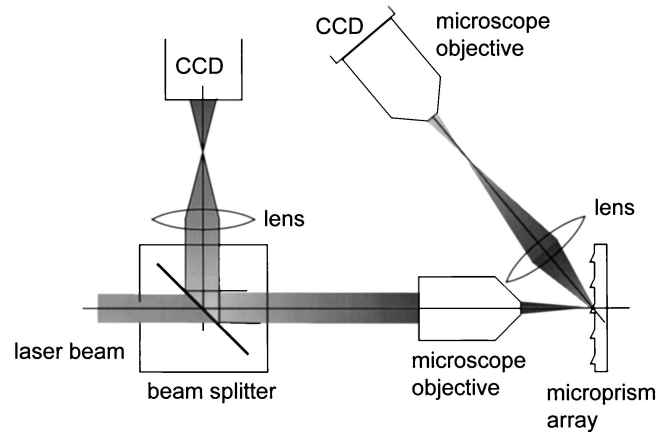


Fig. 5. Optical setup for investigating the effect of the prism surface on the reflected beam.

presented. The reflow process yields a better surface quality. For a reflective prism in quartz glass, we observed an improved focal spot, as shown in Fig. 6(c).

The deflection angle was determined by measurement of the angle of the transmitted beam at the bottom of the glass substrate. By applying Snell's law, we determined the angle inside the glass substrate α to be $\alpha = 1.04^\circ$.

The efficiency of the prisms was also tested. Because of the reflow process the prisms etched into quartz glass yielded good results. With a Hewlett-Packard powermeter, we measured the transmittance of the microprism to be 95% of the transmittance of a flat quartz plate.

4. Microprisms for Planar Optics: Discussion and Conclusion

In this section we discuss the application of microprism couplers for planar optical interconnections. With diffractive coupling elements it is difficult to achieve both a large coupling angle and high efficiency at the same time. On the other hand, both are desirable for various reasons. A high light efficiency of the interconnect reduces requirements on emitter and detector devices, thus simplifying the interconnect and ultimately reducing cost. Large coupling angles are desirable to minimize the number of reflections for achieving a certain lateral-transmission distance. Also, it has been shown that the number of interconnections scales with the coupling angle.⁹ Typically, we want to achieve coupling angles that lie in the range 20°–30°.

There exist two possibilities for the placement of the microprisms: either directly on the GaAs emitter chip or on the top surface of the glass (SiO_2) substrate (Fig. 7). Here we briefly discuss both cases. The deflection angle in the glass substrate with glass prisms [Fig. 7(a)] can be expressed as

$$\alpha = \arctan\left(\frac{h}{l}\right) - \arcsin\left[\frac{1}{n_{\text{qu}}}\sin\left(\arctan\frac{h}{l}\right)\right], \quad (1)$$

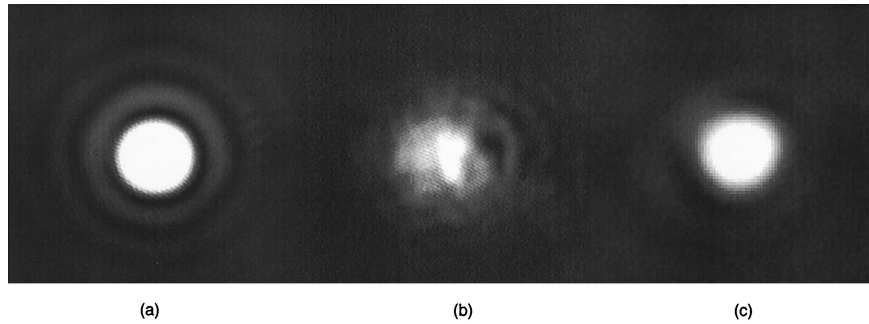


Fig. 6. (a) Airy pattern reflected from a smooth surface. (b) Pattern reflected from a micropism in photoresist. (c) Spot reflected from a micropism in quartz with the reflow technique.

where n_{qu} is the refractive index of the quartz substrate, h is the height of the prism sag, and l is the length of the prism. If the same prism is fabricated in GaAs with n_{GaAs} as the refractive index of GaAs, the deflection angle is

$$\alpha = \arcsin\left(\frac{1}{n_{\text{qu}}}\sin\left\{\arcsin\left[n_{\text{GaAs}}\sin\left(\arctan\frac{h}{l}\right)\right] - \arctan\frac{h}{l}\right\}\right). \quad (2)$$

In Fig. 8 both Eqs. (1) and (2) are plotted versus the aspect ratio $h:l$. It is apparent that the large refractive index of GaAs, $n_{\text{GaAs}} = 3.63$, enables large deflection angles. This also means that etch depths are relatively shallow. For example, a coupling angle of 20° into the glass substrate requires an etch depth of $18\ \mu\text{m}$ for a prism size of $100\ \mu\text{m}$. Internal reflection in the GaAs limits the maximum deflection angle to approximately 40° . In terms of the aspect ratio planar optical interconnects require values of 0.18 to 0.25 for GaAs and 1.4 to 3 for SiO_2 .

A critical issue related to the fabrication of the micropisms (as for other refractive elements) lies in the precision and the reproducibility with which they can be fabricated. Deviations in the fabrication can result from the resist thickness and the resist homogeneity. For example, the mean resist thickness of the AZ4000 series can vary by as much as 6%, which exceeds our tolerable limits, between wafers.³ This problem can be solved by a subsequent oxide RIE process, which is a known technique in VLSI processing. This etch-back process yields an accuracy of the resolution limit of the RIE process that is typically a few nanometers. *In situ* probing with laser interferometry can further improve the deviation to less than 1 nm. The second problem in resist processing is the resist nonuniformity. For a single wafer the resist nonuniformity can be as high as 2% by use of standard processing equipment. Spin coaters equipped with modified chuck covers yield resist nonuniformities of better than 0.05%. During the following RIE process the resist shape is transferred into the substrate. Depending on the etch rates of the resist and the substrate, the resist nonuniformity can be amplified, which means a 0.05%

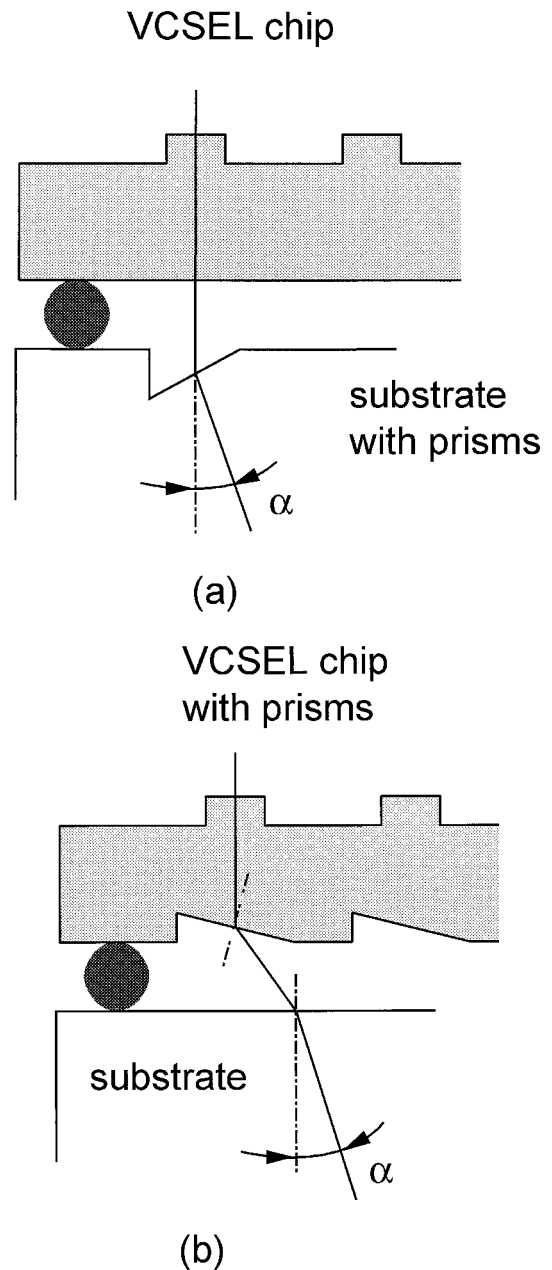


Fig. 7. Deflection angle defined for prisms (a) in GaAs and (b) in quartz.

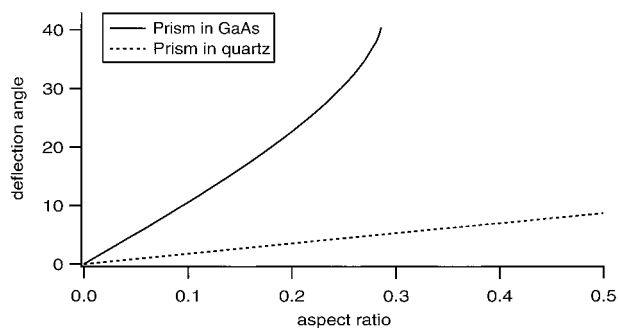


Fig. 8. Deflection angle inside a glass substrate of a planar integrated free-space optical system with a microprism in the bottom of the GaAs substrate or the quartz substrate.

accuracy is not satisfactory. Consequently, further process development is necessary.

Another issue that we would like to mention here is that deviations in the fabrication can be compensated by a tolerant design of the optics. This concept was discussed in connection with planar optical interconnections, for example, in Refs. 2 and 10.

In conclusion, we have reported the first, to our knowledge, results of the fabrication of prism arrays in photoresist and quartz glass by means of analog gray-scale lithography. The optical experiments have demonstrated acceptable surface quality, in particular, in combination with an additional reflow step. An efficiency of 95% has been measured. We hope to apply this technique to realizing light-efficient planar optical interconnections. Further work on the fabrication and the integration of the prisms directly on VCSEL chips is the next step.

References

1. A. Cangellaris, "The interconnect bottleneck in multi-GHz processors: new opportunities for hybrid electrical/optical solu-

tions," in *Proceedings of the Fifth International Conference on Massively Parallel Processing*, L. Johnsson, R. Kostuck, E. Schenfeld, and M. Snir, eds. (IEEE Computer Society, Los Alamitos, Calif., 1998), pp. 98–103.

2. S. Sinzinger and J. Jahns, "Integrated micro-optical imaging system with a high interconnection capacity fabricated in planar optics," *Appl. Opt.* **36**, 4729–4735 (1997).
3. K. Reimer, U. Hofmann, M. Jürss, W. Pilz, H. J. Quenzer, and B. Wagner, "Fabrication of microrelief surfaces using a one-step lithography process," in *Microelectronic Structures and MEMS for Optical Processing III*, M. Motamedi and H. P. Herzig, eds., Proc. SPIE **3226**, 2–10 (1997).
4. E.-B. Kley and W. Dörl, "Einsatz von Elektronenstrahl-lithographie zur Herstellung mikrooptischer Bauelemente," *VDI Ber. (Ver. Dtsch. Ing.)* **960**, 531–541 (1992).
5. W. Däschner, C. Wu, and S. H. Lee, "General aspheric refractive micro-optics fabricated by optical lithography using a high energy beam sensitive glass gray-level mask," *J. Vac. Sci. Technol. B* **14**, 135–138 (1996).
6. M. T. Gale, M. Rossi, L. Stauffer, M. Scheidt, and J. R. Rogers, "Integrated micro-optical systems fabricated by replication technology," in *Diffractive Optics and Micro-Optics*, Vol. 10 of OSA Technical Digest Series (Optical Society of America, Washington, D.C., 1998), pp. 183–185.
7. E. M. Strzelecka, G. B. Thompson, G. D. Robinson, M. G. Peters, B. J. Thibeault, M. Mondry, V. Jayaraman, F. H. Peters, and L. A. Coldren, "Monolithic integration of refractive lenses with vertical cavity lasers and detectors for optical interconnections," in *Optoelectronic Packaging*, M. R. Feldman and Y.-C. Lee, eds., Proc. SPIE **2691**, 45–53 (1996).
8. C. Wu, "Method of making high energy beam sensitive glass," U.S. patent 5,078,771, 7 January 1992.
9. J. Jahns, S. Sinzinger, and M. Testorf, "Scaling considerations for planar optical interconnects," in *Organic Thin Films for Photonic Applications*, Vol. 14 of 1997 OSA Technical Digest Series (Optical Society of America, Washington, D.C., 1997), paper W53.
10. B. Lunitz, and J. Jahns, "Tolerant design of a planar optical clock distribution system," *Opt. Commun.* **134**, 281–288 (1997).